Corrosion protection by organic coatings containing polyaniline salts prepared by oxidative polymerization

M. Kohl[a *], A. Kalendová[a], E. Černošková[a], M. Bláha[b], J. Stejskal[b], M. Erben[a]

[a] Faculty of Chemical Technology, University of Pardubice, 532 10 Pardubice, Czech Republic.

[b] Institute of Macromolecular Chemistry, Academy of Sciences of the Czech Republic, 162 06 Prague 6, Czech Republic.

* Corresponding author: e-mail: Miroslav.Kohl@upce.cz, Phone: +420466037332, Fax: +420466037068, Faculty of Chemical Technology, University of Pardubice, Studentská 95, 532 10 Pardubice, Czech Republic.

Abstract

The aim of this work was to describe the polyaniline salts synthesized and to assess the mechanical and anticorrosion properties of alkyd resin-based coating materials pigmented with them, in dependence on the pigment volume concentration (PVC) and type. Polyaniline salts were prepared by oxidative polymerization in the solutions of inorganic (hydrochloric, phosphoric, and sulfuric) and organic (p-toluenesulfonic and 5-sulfosalicylic) acids. Polyaniline salts were characterized by thermal analysis and spectroscopic methods. Electrical conductivity was also measured by the van der Pauw method and the molecular weight of the polyaniline was determined gel permeation chromatography. Furthermore, the particle size of the solid salts was measured and the morphology was studied by scanning electron microscopy. Subsequently, the parameters required to formulate pigmented organic coatings, i.e. density and critical pigment volume concentration were determined. A soybean oil-based fast drying alkyd resin of medium oil length was used as the binder for the organic coating material. Organic coatings containing the polyaniline salts at pigment volume concentrations 0 %, 1 %, 5 %, 10 % and 15 % were formulated and subjected to a standard accelerated cyclic corrosion tests. The organic coatings (paint films) were also subjected to mechanical tests and to the electrochemical test by potentiodynamic polarization studies.

Keywords: Polyaniline, oxidative polymerization, organic coatings, corrosion.

1. Introduction

Recently, conductive polymers have received considerable attention. Among the important conductive polymers are polyaniline, polypyrrole and polythiophene.[1] Owing to their properties and reasonable preparation costs, such materials have become popular in many branches of science and technology, where the feasibility of using them as substitutes for common metals or other inorganic materials has been studied. Many papers describing their properties as a basis for new uses have been published.[2] Other conductive polymers, such as poly(phenylenediamine), have been investigated to this end as well.[3]

Polyaniline (PANI) can be prepared in five different forms which differ in their oxidation state, chemical structure, color, stability and electrical properties. One of the polyaniline species, green protonated emeraldine (polyaniline salt), is electrically conductive, appreciably more than conventional polymers and nearly as much as semiconductors.[4,5] The structure of the conductive polyaniline species includes an anion, which counterbalances the positive charge of the chain. The anion is derived from the acid used in the protonation process. The acid type and concentration affect polyaniline salt conductivity. Both mineral and organic acids can be used for protonation.[6,7] Previous studies have focused on chemical synthesis and chemical stability.[8-11]

Polyaniline has a potential for advanced applications owing to its outstanding ecological stability, easy preparation and reversible acid/base doping/dedoping chemistry.[12] Thanks to its excellent separation properties, polyaniline finds use in the preparation of membranes for gas separation, pervaporation and electrodialysis.[13] Graphene-polyaniline composites have also attracted much interest as electrode materials for supercapacitors.[14] Recently, functionalized multi-walled carbon nanotubes of a polyaniline nanocomposite have attracted much attention owing to their enhanced electronic properties. They are promising nanocomposites for new applications in chemistry, physics and particularly in the development of new devices such as hydrogen storage, supercapacitors, biosensors, electromechanical actuators, nanoprobes for high-resolution imaging and many more.[15] Furthermore, this conductive polymer has found applications in electronic devices, electrochromic displays, rechargeable batteries, polymer-modified electrodes and biosensors.[16] Polyaniline can be subjected to an oxidation-reduction reaction during which it gains or loses electrons from the surrounding environment; this property may potentially be exploited of in coating materials (paints) by providing enhanced corrosion protection to the base material.[17-19] This polyaniline's ability is made use of for catalytic passivation of iron.[20] Iron is directly oxidised to a ferric state, where ferric oxide is formed and acts as a passivating layer. This direct oxidation process is accelerated by PANI by providing ferric rather than ferrous iron, which is water soluble. The oxidation power of PANI is characterised by the type of doping agent.[20,21]

Accelerated cyclic corrosion tests and electrochemical methods are frequently used to assess the anticorrosion properties of organic coatings. From among electrochemical methods, the potentiodynamic polarization studies is frequently used. This technique enables the polarization resistance (R_p), corrosion potential (E_{cor}), corrosion current density (I_{cor})[22] and corrosion rate (CR)[23] to be determined. The corrosion potential and corrosion current density were determined by analysis of Tafel curves. The polarization resistance was determined from Stern-Geary equation:

$$I_{cor} = \frac{B}{R_p} \tag{1}$$

where the R_p is polarization resistance and B is a constant for the particular system which is calculated from the slopes of the anodic (β_a)and cathodic (β_c) Tafel regions:

$$B = \frac{\beta_a \, \beta_c}{2.303 \, (\beta_a + \beta_c)} \tag{2}$$

Corrosion rate was calculated according to the following equation, where K is constant that defines the units of the corrosion rate, EW is equivalent weight, ρ is density and A is sample area.

$$CR = \frac{I_{cor} \, K \, EW}{\rho \, A} \tag{3}$$

2. Experimental methods

2.1. Synthesis

The synthesis started by preparation of 250 ml of a 0.2 M aniline solution in a 0.8 M solution of an acid, i.e. phosphoric acid (H_3PO_4), sulfuric acid (H_2SO_4), hydrochloric acid (HCl), *p*-toluenesulfonic acid (PTSA) or 5-sulfosalicylic acid (SSA). A 0.25 M solution of ammonium peroxodisulfate (250 ml) was also prepared. Both solutions were mixed and and stirred for 60 min. The polymerization process was accompanied by a color change. After 24 hours, the polymerization product was separated by filtration on Buchner funnel and rinsed with a dilute solution of the acid that was used for synthesis, followed by acetone. The rinsed product

was allowed to dry in air for 24 h and then dried at 60 °C in a drier. Five polyaniline salt types were thus prepared: PANI-H_3PO_4, PANI-H_2SO_4, PANI-HCl, PANI-PTSA, and PANI-SSA.

2.2. Characterization

The thermogravimetric analyses (TGA) were performed using a DMA, D047 (RMI). The measurements were carried out in air between 30 and 600°C at a heating rate of 5 °C.min^{-1}.

The calorimetric measurements were performed by calorimeter (Mettler DSC 12E) in perforated alumina pans using heating rate 5 °C.min^{-1} in the temperature range 30-525 °C. The calorimeter was calibrated with indium and sapphire. Samples were weighed (Sartorius R 160 P) before and after DSC measurements.

X-ray diffraction (XRD) data were obtained with D8-Advance (Bruker AXE) diffractometer with Bragg–Brentano θ–θ geometry using CuK_α radiation. XRD data were collected at room temperature from 5 to 70° (2θ) in 0.02° steps with a counting time of 3 s per step.

Transmission IR spectra were recorded in the 4000–400 cm^{-1} region on a Nicolet 6700 FTIR spectrometer in KRS-5 pellets. Pellets were dried in a desiccator over P_2O_5 for 3 days before measurements.

Gel permeation chromatography for measurement of molecular mass of the polyanilines was performed on a Calc 100 (Labio, Czech Republic) chromatograph equipped with a PLgel mixed-C column (Polymer Laboratories, UK) using *N*-methylpyrrolidone containing 0.005 g.cm^{-3} of lithium bromide (to prevent aggregation) as the eluent at the flow rate of 0.70 ml.min^{-1}. Samples were dissolved in mobile phase containing 0.005 g.cm^{-3} of triethanolamine (for sample deprotonation). The system was calibrated with polystyrene standards. Samples were detected spectrophotometrically at 340 nm.

Conductivity was determined by a four-point van der Pauw method using a Keithley 237 High-Voltage Source Measurements Unit and a Keithley 2010 Multimeter equipped with a 2000-SCAN 10 Channel Scanner Card on samples compressed into pellets, 13 mm in diameter and ca. 1 mm thick.

Determination of particle size and the distribution of pigment particle size were identified by means of Mastersizer 2000 (Malvern, Instruments Ltd., UK), which is able to measure the distribution of particles sized from 0.01 to 2000 μm. The pigment particle surface and shape were examined using a JEOL-JSM 5600 LV scanning electron microscope (JEOL, Japan).

The pH of the aqueous extracts was determined as described in ISO 789-9. Suspensions (10 wt.%) of the pigments in redistilled water were prepared and the pH was measured continually for 21 days until a steady value was observed. The suspension was then filtered off and the final filtrate pH was measured with a WTW pH 320 Set-2 multiprocessor pH meter fitted with a measuring glass electrode (WTW Wissenschaftliche Werkstätten, Germany). The specific electric conductivity of the aqueous suspensions was measured conductometrically with a Handylab LF1 conductometer (Schott–Geräte GmbH, Germany) in combination with a measuring Pt cell.

2.3. Formulation and preparation of the organic coatings

The critical pigment volume concentration (CPVC) of the pigments was calculated from the density (determined using Autopycnometer Micromeritics 1320) and oil absorption (determined according to the Czech State Standard 67 0531 using the "pestle – mortar" method).[24] The binder for the organic coatings was an alkyd resin whose technical data are

shown in Table 1. The organic coatings contained the polyaniline salts at pigment volume concentrations (PVC) 0 %, 1 %, 5 %, 10 %, and 15 %. These model organic coatings neither contain other pigments nor fillers in order to evaluate the action of polyaniline salts in organic coatings. Formulations of Organic Coatings pigmented by polyaniline salts prepared in the environment of inorganic acids are shown in Table 2. Formulations of Organic Coatings pigmented by polyaniline salts prepared in organic acids are shown in Table 3. Organic coatings were dispersed using a Disolver-type equipment at 4,000 r.p.m. for 40 minutes.To harden the organic coatings there were used common cobalt-based driers, such as cobalt(II) 2-ethylhexanoate (Co-Nuodex) which were added in the quantity of 0.1% as expresed for 100 % alkyd resin. Once prepared, the paints were applied to steel panels (standard S-36 low-carbon steel panels, Q-Lab Corporation) using an applicator with a slit (200 µm) and the dry film thickness (DFT) was measured with a magnetic gauge as per ISO 2808.[25]

Paint films (PVC = 15 %) had been prepared on a polyethylene sheet then removed after drying, cut into 1 mm × 1 mm pieces and used to prepare 10 wt.% aqueous suspensions of the films. pH and specific electric conductivity were measured continually for 21 days until a steady value had been observed. The suspensions were then filtered off and the pH of the final filtrate and specific electric conductivity were measured.

Table 1 Technical data of the alkyd resin serving as the binder.

Trade name /manufacturer:	CHS – Alkyd S 471x60, Spolchemie a.s., Ústí nad Labem, Czech Republic
Composition:	Soybean-based air-drying medium oil alkyd resin, supplied as a 60 % (low-viscosity) solution in xylene, oil length 47 %.
Technical data:	Density: 1.01 g.cm^{-3} Acid number: ≤ 6 mg KOH/g Viscosity: 0.8 – 1.7 Pa.s (25 °C) Dry matter: 60 % Solvent: xylene

Table 2 Formulation of organic coatings containing PANI-H_3PO_4, PANI-H_2SO_4 and PANI-HCl.

PVC [%]	Formulation of organic coatings containing PANI-H_3PO_4		Formulation of organic coatings containing PANI-H_2SO_4		Formulation of organic coatings containing PANI-HCl	
	Alkyd resin [wt. %]	PANI-H_3PO_4 [wt. %]	Alkyd resin [wt. %]	PANI-H_2SO_4 [wt. %]	Alkyd resin [wt. %]	PANI-HCl [wt. %]
1	99.14	0.86	99.08	0.92	99.21	0.79
5	95.86	4.14	95.39	4.61	96.02	3.98
10	91.29	8.71	90.75	9.25	91.95	8.05
15	86.84	13.16	86.07	13.93	87.78	12.22

Table 3 Formulation of organic coatings containing PANI-PTSA and PANI-SSA.

PVC [%]	Formulation of organic coatings containing PANI-PTSA		Formulation of organic coatings Containing PANI-SSA	
	Alkyd resin [wt. %]	PANI-PTSA [wt. %]	Alkyd resin [wt. %]	PANI-SSA [wt. %]
1	99.20	0.80	99.09	0.91
5	95.96	4.04	95.42	4.58
10	91.84	8.16	90.81	9.19
15	87.63	12.37	86.15	13.85

2.4. Mechanical properties of the paints

The paints were subjected to tests providing information on the paint film elasticity and strength. Adhesion of the films to the substrate was assessed on cutting a lattice into the films as per ISO 2409, by using a special cutting blade with cutting edges 2 mm apart. The impact strength of the paint films applied to steel panels was determined by letting a 1000 g weight fall onto the panels from different heights and recording the largest height (in mm) at which the film integrity remained undisturbed (ISO 6272). The paint film resistance to cupping was evaluated by measurement on an Erichsen cupping tester. The result is the steel ball indentation depth (in mm) at which the film integrity remained undisturbed, as specified in ISO 1520. The test aimed at evaluating the paint film resistance to bending consists in bending the painted panels over mandrels of different diameter and recording the largest diameter (in mm) at which the paint film integrity is disturbed, as specified in ISO 1519.

2.5. Corrosion studies

Accelerated corrosion tests are based on the intensification of the effects of natural forces that have a decisive influence on the protective properties of the paints, their degradation, and primarily on the extent of corrosion under the paint film on a protected base.

The exposure of the samples in a testing chamber was performed in 12-h cycles divided into three parts: 6 h of exposure to a mist of a 5 % solution of NaCl at a temperature of 35 °C, 2 h of exposure at a temperature of 23 °C and 4 h of humidity condensation at a temperature of 40 °C (ISO 9227). The samples were evaluated after 576 h of exposure.

The exposure of the samples in a testing chamber was performed in 24-h cycles: 8 h of exposure to SO_2 at a temperature of 35 °C (1 l SO_2 is injected into 300 l chamber) followed by exposure to the condensation of humidity for a period of 16 hours and at a temperature of 21 °C (ISO 6988). The condition of the samples was evaluated after 1632 h of exposure.

The corrosion effects after completion of the tests were evaluated as specified in the above standards. Blistering on the paint film surface was assessed by comparing with the photographs of standards included in the ASTM D 714-87 standards. Corrosion on the metal plane was evaluated (after stripping the paint film down) by comparison with the photographs of standards included in the ASTM D 610-85 standard.[26]

ASTM D 714-87 method

The method classifies the osmotic blisters according to their size designated by figures of 2, 4, 6, and 8 (2 denotes the largest size, and 8 the smallest one). An information on the frequency of occurrence is given. The highest occurrence of blisters is designated as D (dense), the other ones as MD (medium dense), M (medium) and F (few). In such a way a series from the surface area attacked at least by the osmotic blisters up to the heaviest occurrence can be formed as follows: 8F–6F–4F–2F–8M–6M–4M–2M–8MD–6MD–4MD–2MD–8D–6D–4D–2D.[26]

ASTM D 610-85 method

The results obtained by means of this method are related to the degree of corrosion in area under the protective coating. The result is thus a definite corrosion degree of the substrate surface expressed in percents (0 – 0,01 – 0,03 – 0,1 – 0,3 – 1 – 3 – 10 – 16 – 33 – 50 – 100 %).[26]

The corrosion resistant properties of the coating were evaluated using potentiodynamic polarization studies. For measurements was used a conventional three-electrode cell assembly. A platinum foil was used as the counter electrode and a saturated calomel electrode was used as the reference electrode. The assembly was connected to potentiostat/galvanostat (VSP - 300, France). A machine was used to ensure that 1 cm^2 of the coating was exposed in a 3.5 wt.%

NaCl solution. The paint films were exposed to the NaCl solution for 12 hours, after which they were measured by the potentiodynamic polarization studies. The polarization region was from -10 mV/E_{OC} to +10 mV/E_{OC} at a rate of 0.166 mV/s.

3. Results and discussion

3.1. Thermogravimetric analysis

The samples were examined by TGA. The TGA traces of the various polyaniline salt types were nearly identical. All exhibited three regions where weight loss took place. The weight loss data are given in Table 4. The first weight loss amounting to 2–6.3 %, taking place at temperatures up to 175 °C, was attributed to the loss of moisture and of adsorbed low molecular weight substances. A next, very small weight change (≤1 %) was observed within the temperature region from 175 °C to 250 °C. The third weight loss, very marked (>76 %), was observed within the temperature region from 250 °C to 600 °C, where the sample underwent thermo-oxidative degradation.[27,28] The weight loss observed at 600 °C was > 83 % for all of the polyaniline salts synthesized.

Table 4 Temperature range and mass loss for the polyaniline salts.

Polyaniline salt	**Loss mass** (T: 50 – 175°C) **[%]**	**Loss mass** (T: 175 – 250°C) **[%]**	**Loss mass** (T: 250 – 600°C) **[%]**	**Residual [%]**
PANI-H_3PO_4	2.9	1.0	84.9	11.2
PANI-H_2SO_4	4.1	1.0	78.9	16.0
PANI-HCl	2.8	0.9	82.4	13.9
PANI-PTSA	2.0	0.2	85.5	12.3
PANI-SSA	6.3	0.6	76.1	17.0

3.2. Differential scanning calorimetry (DSC)

The samples were examined by differential scanning calorimetry. The DSC spectra up to T = 525 °C are shown in Fig. 1, the enthalpy values (ΔH) of the endothermic and exothermic changes are displayed in Table 5. The DSC spectra of the various polyaniline salt types were nearly identical. All samples exhibited an endothermic change within the region from 75 °C to 175 °C. This endothermic change can be linked to the weight loss observed in thermogravimetry and attributed to the loss of moisture and adsorbed low-molecular-weight substances. This is supported by the enthalpy data. An exothermic change which is attributed to crosslinking or recrystallization[29] was observed in the DSC spectra within the range from 175 °C to 275 °C. This interpretation is also supported by the thermogravimetry data, where a negligible weight change occurred within that temperature range. A marked exothermic change was observed within the temperature range from 275 °C to 525 °C on the DCS traces of all the polyaniline salts examined; this was attributed to thermo-oxidative degradation.[27] Once again, this is in accordance with the results of the thermogravimetric analysis, where a marked (>76 %) weight loss was observed within the temperature range in question.

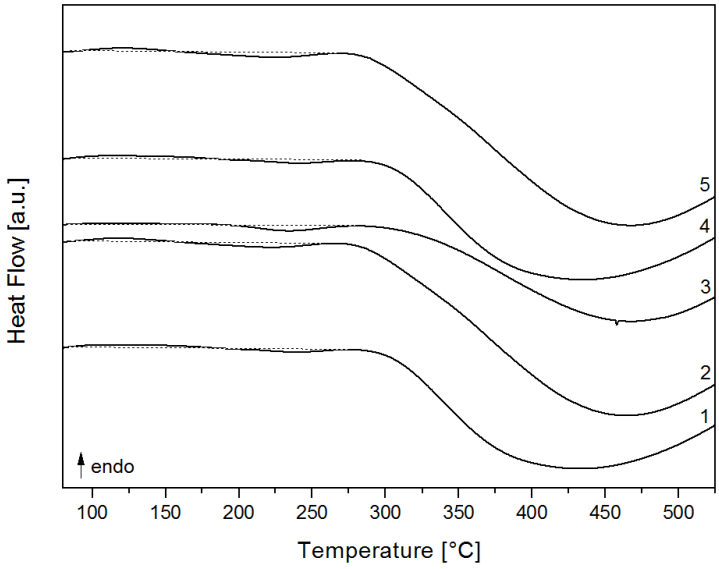

Fig. 1. DSC spectra of the polyaniline salts (1. PANI-H_3PO_4, 2. PANI-H_2SO_4, 3. PANI-HCl, 4. PANI-PTSA, 5. PANI-SSA)

Table 5 Enthalpies of the endothermic and exothermic changes derived from the DSC spectra.

Polyaniline salt	Tp [°C]	ΔH [J.g^{-1}]	Tp [°C]	ΔH [J.g^{-1}]
PANI-H_3PO_4	115	17	218	-13
PANI-H_2SO_4	105	16	215	-6
PANI-HCl	117	8	226	-19
PANI-PTSA	108	9	234	-11
PANI-SSA	110	10	212	-21

3.3. X-ray diffraction analysis

The X.ray diffractograms of polyaniline salts are shown in Fig. 2. This figure reveals thatPANI-H_3PO_4 and PANI-H_2SO_4 have two peaks at 2θ around 20° and 25°, and PANI-HCl, PANI-PTSA and PANI-SSA have three peaks at 2θ around 14°, 20° and 25°. They had a similar profile to that of free PANI reported in literature.[30] Considering these peaks, the one of 2θ around 25° may be ascribed to periodicity perpendicular to the polymer chain. The other peaks may be caused by the branches of the doping agents which were doped in the PANI chains at various locations.[31]

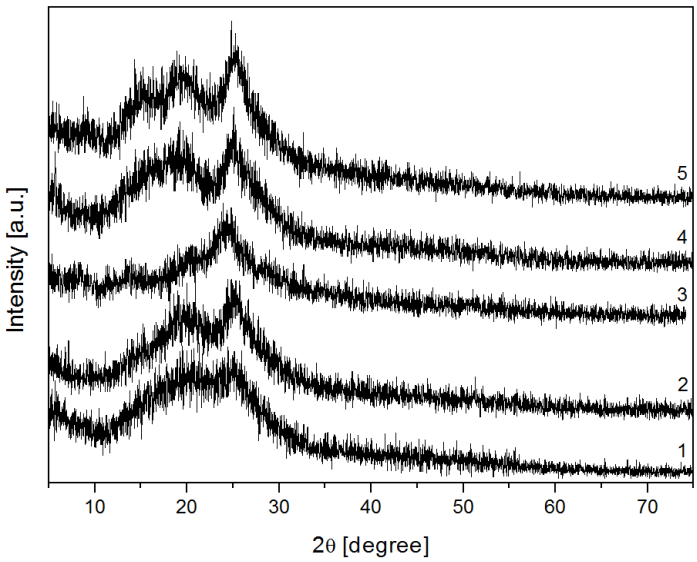

Fig. 2. XRD diffractograms of the polyaniline salts (1. PANI-H_3PO_4, 2. PANI-H_2SO_4, 3. PANI-HCl, 4. PANI-PTSA, 5. PANI-SSA)

3.4. Infrared spectroscopy

The compounds were studied by FTIR spectroscopy in the range of 4000-600 cm^{-1}. All prepared PANI samples showed medium bands at 3449, 3231, 3060 cm^{-1} corresponding to stretching vibrations of OH, NH and aromatic CH bonds, respectively. Although the band at ~3449 cm^{-1} has been previously assigned to free NH stretching vibrations,[32,33] we believe that this band must be associated with OH group stretching mode. We have two arguments to support this statement. First, heating of PANI samples to 150 °C (removal of moisture and physisorbed water molecules) caused this band to disappear. Secondly, in the SSAe of PANI-SSA, the band at 3441 cm^{-1} was significantly stronger than the band at 3239 cm^{-1} due to its strengthening by the presence of phenolic OH groups involved in intramolecular H-bonds. For the purpose of comparison, we also measured the IR spectrum of SSA sodium salt, showing significant absorption at 3432 cm^{-1}. Heating of PANI-SSA to 150 °C led to only a slight decrease in the intensity of this band, as SSA and its salts are stable up to 200 °C. In the IR spectra of PANI-SSA, we also detected C=O stretching bands of the carboxylic acid functional group at 1674 cm^{-1} (1672 cm^{-1} in the SSA sodium salt).

Figure 3 shows the spectra of PANI salts in the region of 1800–600 cm^{-1}, where bands characteristic for polyaniline salts are present.[34] The observed bands, together with their assignment (based on the comparison with reported data)[33,35] are listed in the Table 6. The vibrational pattern in this region was similar for all the studied PANI samples and, upon comparing the IR spectra, we could distinguish the bands corresponding to anions (sulfate, sulfonate or dihydrogen phosphate) incorporated into the PANI salts during synthesis.[36,47]

In the SSAe of PANI-H_3PO_4 and PANI-SSA, weak absorption at 1373 cm^{-1} was found, typical of the PANI base (C–N stretching in the neighborhood of a quinonoid ring).[32] The presence of this band indicates that the PANI salt was not fully protonated, which also correlates with the lower conductivity observed for these two samples (see below).

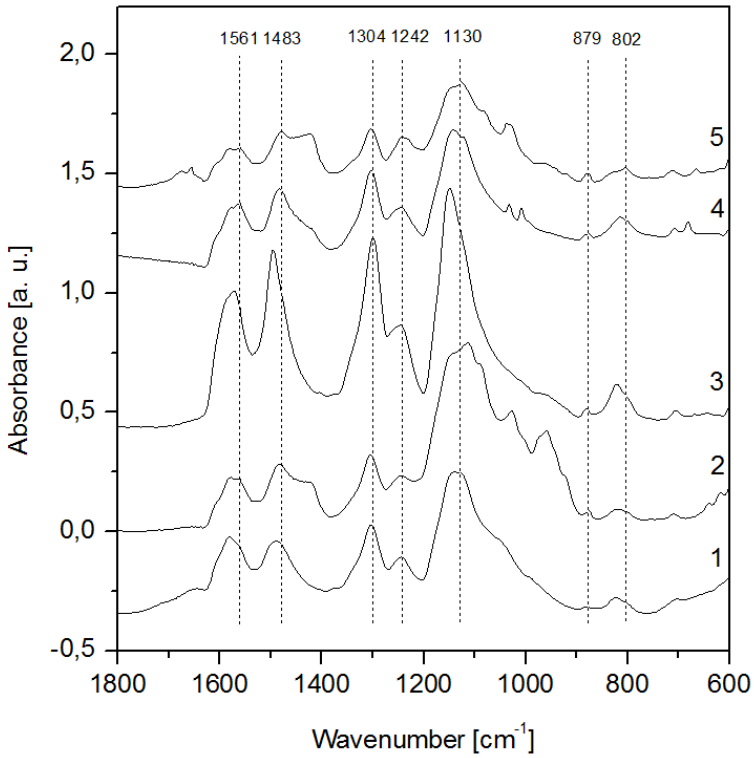

Fig. 3. FTIR spectra of the polyaniline salts (1. PANI-H_3PO_4, 2. PANI-H_2SO_4, 3. PANI-HCl, 4. PANI-PTSA, 5. PANI-SSA).

Table 6

The assignment of FTIR bands for the studied polyaniline salts.

Mode	Wavenumber [cm^{-1}]				
	PANI-H_3PO_4	**PANI-H_2SO_4**	**PANI-HCl**	**PANI-PTSA**	**PANI-SSA**
Quinonoid (Q) ring stretching	1567	1557	1556	1556	1574
Benzenoid (B) ring stretching	1484	1472	1471	1473	1477
(C–N) of secondary aromatic amine	1298	1295	1289	1295	1299
($C–N^{\bullet+}$) in the polaron lattice of PANI	1242	1240	1236	1228	1225
$Q=NH^{+}–B$ or $B–NH^{+\bullet}–B$	1109	1105	1105	1112	1109
γ (C–H) 1,2,4-trisubstituted ring /B ring deformation	879	878	878	878	878
γ (C–H) (1,4-disubstituted ring)/Q ring deformation	795	788	791	792	802
ν (S–O)	–	1090, 1026, 1006	–	1142, 1033, 1008	1126, 1084, 1034
ν (P–O)	1048, 1092	–	–	–	–

B: benzenoid ring; Q: quinonoid ring; γ: out-of-plane deformation.

3.5. Molecular weight

The observed molecular weights of the polyaniline salts are provided in Table 7. The PANI-PTSA salt dissolved completely during the determination, whereas the remaining polyaniline salts dissolved only partially. The polyaniline salts that were prepared in mineral acid solutions exhibited polydispersity index levels from 3.2 to 3.9 and molecular weights from 7,000 to 14,000, whereas the polyaniline salts that were prepared in organic acid solutions exhibited polydispersity index levels from 4.0 to 4.8 and molecular weights from 13,000 to 25,000. Previous reports[38] have provided lower polydispersity index levels, i.e. 2.0–3.1, and comparable molecular weight data for the polyaniline salts.

Table 7 Molecular weight, polydispersity index, conductivity, and average particle size of polyaniline salts.

Polyaniline salt	M_w	M_w/M_n	Conductivity [S.cm^{-1}]	Particle size [µm]
PANI-H_3PO_4	7000	3.2	0.13	4.1 ± 0.1
PANI-H_2SO_4	10000	3.5	1.48	4.0 ± 0.1
PANI-HCl	14000	3.9	1.75	4.0 ± 0.1
PANI-PTSA	25000	4.8	5.85	3.9 ± 0.1
PANI-SSA	13000	4.0	0.78	3.9 ± 0.1

3.6. Conductivity

The electrical conductivity of PANI-H_3PO_4 was markedly lower than the conductivities of the remaining polyaniline salts (Table 7). This can be explained in terms of incomplete protonation of the salt in question, as found by FTIR spectroscopy. Incomplete protonation was also observed for PANI-SSA, whose conductivity was also lower than the conductivities of the fully protonated polyaniline salts. Differences between the electrical conductivity levels were also observed between the fully protonated polyaniline salts: conductivity decreased in the order PANI-PTSA > PANI-HCl > PANI-H_2SO_4. This order may be linked to the molecular weight (M_w), which increased in that order. The observed electrical conductivity values were within the range found for polyaniline salts prepared by oxidative polymerization.[34] Note that the electrical conductivity of the non-conductive polyaniline species (emeraldine base) is 1×10^{-8} S.cm^{-1}.[39]

3.7. Particle size

The mean particle size (Table 7), identified with the diameter of an equivalent sphere, i.e. a sphere that scatters laser radiation to the same extent as the particle measured) of the polyaniline salts was from 3.9 µm to 4.1 µm.

3.8. Particle morphology

Microphotographs of the polyaniline salts are shown in Fig. 4. The photographs were primarily used to examine the shape and surface of the substances studied. The microphotographs demonstrate that the polyaniline salts had an isometric shape and formed clusters of particles.

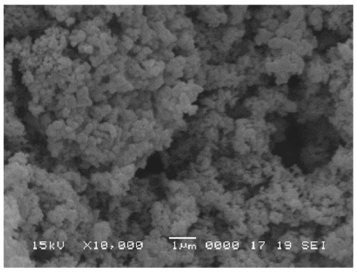

1.

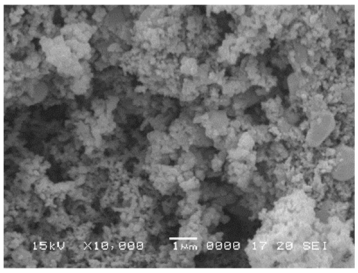

2.

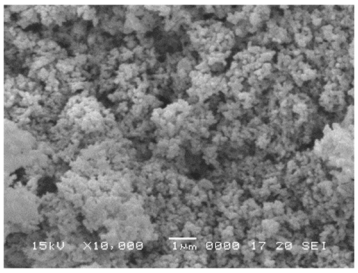

3.

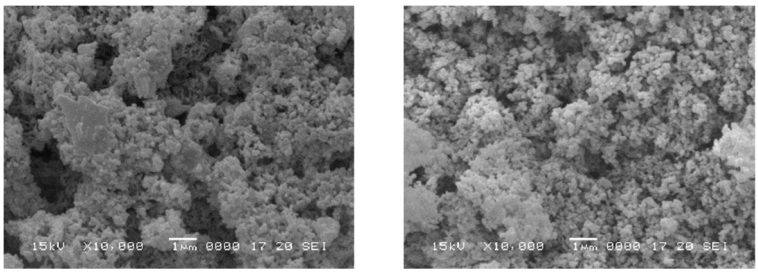

4. 5.

Fig. 4. Microphotographs of the polyaniline salts (1. PANI-H_3PO_4, 2. PANI-H_2SO_4, 3. PANI-HCl, 4. PANI-PTSA, 5. PANI-SSA).

3.9. pH and electrical conductivity of aqueous extracts of the polyaniline salts and paint films

The pH and and electrical conductivity data for aqueous extracts of the polyaniline salts, measured over a period of 21 days, are given in Table 8. The systems were prepared by suspending 10 % (w/w) of the polyaniline salts in redistilled water at an initial pH of 6.50 and electrical conductivity 1.5 $\mu S.cm^{-1}$. All of the suspensions exhibited a substantial increase in acidity (to pH < 2) and electrical conductivity over 21 days. The highest electrical conductivity was found for PANI-H_2SO_4, i.e. 63.25 $mS.cm^{-1}$. This salt also exhibited the greatest increase in acidity, i.e. to pH 1.35. This increase in both acidity and electrical conductivity can be explained in terms of the deprotonaction of the polyaniline salts.[40]

Binders based on alkyd resins dry due to oxidative polymerisation mechanism yielding a solid insoluble polymeric film.[41] The pH and electrical conductivity data for aqueous extracts of the paint films measured over a period of 21 days, are given in Table 8. The pH of the unpigmented paint film leachate amounted to 3.7 and the pH of the paint films leachate (PVC = 15%) showed slightly lower values (3.4 to 3.6). The electrical conductivity of the leachate prepared from unpigmented paint film was 273.87 $mS.cm^{-1}$ and electrical conductivity of the leachate obtained from pigmented paint films (PVC = 15%) achieved slightly higher values (280.45 to 302.56 $mS.cm^{-1}$). From the results of exposure of paint films containing polyaniline salts in the aqueous environment is thus apparent that there is a deprotonation of the insoluble polymer film (as opposed to the direct exposure of polyaniline salts in powder form in an aqueous medium). Significant reduction of pH and conductivity increase can be expected in coatings which are pigmented to PVC > CPVC.[42] In this study, however, coatings were tested with peak values equaling PVC = ½ CPVC.

Table 8 pH and electrical conductivity of aqueous suspensions of the polyaniline salts and the paint films over a period of 21 days.

Polyaniline salt	Aqueous extracts of the polyaniline salts		Aqueous extracts of the paint films (PVC = 15 %)	
	pH [21]	Electric conductivity [21] [$mS.cm^{-1}$]	pH [21]	Electric conductivity [21] [$mS.cm^{-1}$]
PANI-H_3PO_4	1.86 ± 0.01	18.29 ± 0.5 %	3.52 ± 0.01	285.12 ± 0.5 %
PANI-H_2SO_4	1.35 ± 0.01	63.25 ± 0.5 %	3.41 ± 0.01	302.56 ± 0.5 %
PANI-HCl	1.92 ± 0.01	16.31 ± 0.5 %	3.56 ± 0.01	296.86 ± 0.5 %
PANI-PTSA	1.74 ± 0.01	13.42 ± 0.5 %	3.61 ± 0.01	280.45 ± 0.5 %
PANI-SSA	1.82 ± 0.01	18.12 ± 0.5 %	3.58 ± 0.01	289.37 ± 0.5 %

3.10. Density, oil absorption and critical pigment volume concentration (CPVC)

The basic parameters of the polyaniline salts are provided in Table 9. The densities of the salts were within the range of 1.37–1.57 g.cm^{-3}. The relatively low densities suggest that the sedimentation rate in organic coating materials will not be high. This hypothesis was verified experimentally by a 120-day storability/stability test during which the samples were kept at room temperature. No gel formation or appreciable viscosity change in the organic coating materials was observed during the test. The CPVC values of the polyaniline salts lay within the range from 27.9 % to 30.5 %. The CPVC depends on density and on the oil absorption, the latter providing indirect information on the pigment's specific surface area, particle size distribution and porosity. Knowledge of the CPVC is a prerequisite for appropriate formulation of the pigmented organic coating material.[43]

Table 9 Densities, oil absorption and CPVC levels of the polyaniline salts.

Polyaniline salt	Density [g.cm^{-3}]	Oil absorption [g.100 g^{-1}]	CPVC [%]
PANI-H_3PO_4	1.47 ± 0.02	152	28.9
PANI-H_2SO_4	1.48 ± 0.02	159	27.9
PANI-HCl	1.37 ± 0.02	153	30.3
PANI-PTSA	1.37 ± 0.02	152	30.5
PANI-SSA	1.57 ± 0.02	156	27.1

All the parameters are given as arithmetic averages within 10 measured values.

3.11. Mechanical properties of the coating systems

The results of the mechanical tests, listed in Table 10, were used to assess the mechanical resistance of the organic coatings. The data demonstrate that neither the polyaniline dopant type nor the pigment volume concentration has an adverse impact on the organic coatings' mechanical properties when compared to the nonpigmented organic coating; a slight decrease in mechanical resistance was only observed at PVC = 15 %. At this PVC, adhesion was only degree 2, compared to degree 1 at lower PVC levels. Also, formation of microcracks was observed on bending the coated panel over a mandrel 6 mm in diameter, whereas no microcracks appeared even if the panel was bent over a mandrel having the lowest diameter of 4 mm if the PVC was lower than 15 %. Similarly, in the impact test, the organic coating with PVC = 15 % exhibited microcracks if the weight was dropped from a 95 cm height, whereas no microcracks were observed on organic coatings with lower PVC levels if the weight was dropped from a 100 cm height. And similarly, the cupping test on coatings with PVC = 15 % exhibited microcracks at a cupping depth of 9.5 mm, in contrast to coatings with lower PVC levels exhibiting no microcracks at a cupping depth of 10 mm. (In fact, the 10 mm depth was limiting for the steel panel used because this panel itself cracked if larger cupping depths, 11-12 mm, were applied).

Table 10 Results of the mechanical tests, DFT = 60 ± 10 μm.

Sample	PVC [%]	Adhesion test [dg.]	Bend test [mm]	Impact test [cm]	Cupping test [mm]
PANI-H_3PO_4	0	1	< 4	> 100	> 10
	1	1	< 4	> 100	> 10
	5	1	< 4	> 100	> 10
	10	1	< 4	> 100	> 10
	15	2	< 6	95	9.0
PANI-H_2SO_4	0	1	< 4	> 100	> 10
	1	1	< 4	> 100	> 10
	5	1	< 4	> 100	> 10

	10	1	< 4	> 100	> 10
	15	2	< 6	95	9.0
	0	1	< 4	> 100	> 10
	1	1	< 4	> 100	> 10
PANI-HCl	5	1	< 4	> 100	> 10
	10	1	< 4	> 100	> 10
	15	2	< 6	95	9.0
	0	1	< 4	> 100	> 10
	1	1	< 4	> 100	> 10
PANI-PTSA	5	1	< 4	> 100	> 10
	10	1	< 4	> 100	> 10
	15	2	< 6	95	9.0
	0	1	< 4	> 100	> 10
	1	1	< 4	> 100	> 10
PANI-SSA	5	1	< 4	> 100	> 10
	10	1	< 4	> 100	> 10
	15	2	< 6	95	9.0

All the parameters are given as arithmetic averages within 10 measured values.

3.12. Accelerated cyclic corrosion tests

The results indicating resistance of the organic coatings to a salt mist atmosphere are given in Table 11. The organic coatings were exposed to the corrosive environment for 576 hours. Two types of corrosion effects were examined: corrosion in the panel area and the formation of blisters.

The organic coatings with PANI-H_3PO_4 as the pigment exhibited the highest resistance to corrosion effects at PVC = 5 %. Corrosion over the panel area was increased (3 %) if the PVC was increased to 15 %. The coating with PANI-H_2SO_4 also exhibited the highest corrosion resistance at PVC = 5 %, whereas at PVC = 15 % the corrosion effect in the panel area was appreciably greater. The highest resistance was observed at PVC = 5 % for the organic coatings with PANI-HCl, which exhibited 0.03 % corrosion in the substrate area and no development of blisters. Corrosion in the panel area was appreciably higher at PVC = 10 % and 15 %. The organic coatings containing the pigment PANI-PTSA displayed high corrosion resistance at PVC = 1 – 10 %: corrosion in the panel area was at the level of 0.01 - 0.03 % and no blisters were observed. Corrosion in the panel area was higher at PVC = 15 %. The results for the organic coatings containing PANI-SSA were identical to those observed for the coatings with PANI-PTSA.

Hence, the organic coatings with the polyaniline salts exhibited the highest resistance to corrosion effects if the pigment volume concentration was 5 %. Among the polyaniline salts used as pigments in the organic coatings, those synthesized in acids (H_3PO_4, PTSA and SSA) provided the highest corrosion resistance. The corrosion resistance was invariably poorer if the PVC level was increased to 15 %. This fact can be explained in terms of a reduced barrier effect provided by the organic coatings. A reduced barrier effect means that aggressive media can penetrate more easily through the coating and attack the initially protected substrate. This effect has been observed before in studies on the anticorrosion efficiency of polyaniline salts.[44]

Table 11 Results of the corrosion test in a salt mist atmosphere. Exposure for 576 hours, DFT = 90 ± 10 µm

Sample	PVC	Blistering	Corrosion
	[%]	Metal base [dg]	Metal base [%]
PANI-H_3PO_4	0	2F	0.3
	1	4M	0.03
	5	6F	0.01
	10	6M	0.01
	15	4M	3
PANI-H_2SO_4	0	2F	0.3
	1	6F	0.1
	5	-	0.1
	10	4M	0.3
	15	4F	16
PANI-HCl	0	2F	0.3
	1	-	0.3
	5	-	0.1
	10	4M	3
	15	4M	10
PANI-PTSA	0	2F	0.3
	1	-	0.03
	5	-	0.01
	10	-	0.03
	15	6F	1
PANI-SSA	0	2F	0.3
	1	-	0.03
	5	-	0.01
	10	-	0.03
	15	6F	1

All the parameters are given as arithmetic averages within 10 measured values.

The results indicating resistance of the organic coatings to an atmosphere with SO_2 are summarized in Table 12. The organic coatings were exposed to the corrosive environment for 1632 hours. Two types of corrosion effects were examined: corrosion in the panel area and the formation of blisters.

No appreciable effect of the polyaniline salt type was observed in the accelerated corrosion test on panels coated with the paint films containing different polyaniline salts. Blisters were never observed and corrosion of the steel panel beneath the coating never exceeded 0.03 % if the polyaniline salt was present at PVC = 1 % – 10 %. However, if the PVC was increased to 15%, blisters were found on the film and corrosion on the steel panel exceeded 0.1 %. The non-pigmented organic coating also exhibited blisters in this test.

From the above results of cyclic corrosion tests it is apparent that the highest corrosion resistance has been achieved by the organic coating containing PANI-PTSA (PVC = 5 %) and by the organic coating containing PANI-SSA (PVC = 5 %).

Table 12 Results of the corrosion test in an atmosphere with SO_2. Exposure for 1632 hours, DFT = 90 ± 10 µm

Sample	PVC	Blistering	Corrosion

	[%]	Metal base [dg]	Metal base [%]
PANI-H_3PO_4	0	6M	0.03
	1	-	0.01
	5	-	0.01
	10	8M	0.03
	15	8M	0.1
PANI-H_2SO_4	0	6M	0.03
	1	-	0.01
	5	-	0.01
	10	-	0.03
	15	8M	0.1
PANI-HCl	0	6M	0.03
	1	-	0.01
	5	-	0.01
	10	-	0.03
	15	8M	0.1
PANI-PTSA	0	6M	0.03
	1	-	0.01
	5	-	0.01
	10	-	0.03
	15	8F	0.1
PANI-SSA	0	6M	0.03
	1	-	0.01
	5	-	0.01
	10	-	0.03
	15	8F	0.1

All the parameters are given as arithmetic averages within 10 measured values.

The organic coatings were exposed to a 3.5 wt.% NaCl solution for 12 hours and then measured by the potentiodynamic polarization studies. The corrosion potential (E_{cor}), corrosion current density (I_{cor}), Tafel slopes (β_a, β_c), polarization resistance (R_p) and corrosion rate (CR) were measured for each coating, and different values were obtained for the different coatings. The results are listed in Table 13.

The results indicating corrosion rates were lowest and the polarization resistance highest if the polyaniline salt was present in PVC = 1 % or 5 % whereas the corrosion rate was one order of magnitude higher and the polarization resistance was lower if the PVC was increased to 10 % or 15 %; such corrosion rates and polarization resistance levels approach those exhibited by the non-pigmented organic coatings. Moreover from the results of this study it is apparent that the highest values of polarization resistance was reached by the organic coating containing the PANI-SSA pigment (PVC = 5 %). Slightly lower polarization resistance was reached by the organic coating containing the PANI-H_2SO_4 pigment (PVC = 5 %). The corrosion rates shown by these coatings were the lowest in comparison with other tested organic coatings.

Table 13 Results of the obtained from potentiodynamic polarization curves, DFT = 90 ± 10 μm.

Sample	PVC [%]	E_{cor} [mV]	I_{cor} [μA/cm²]	β_a [mV]	β_c [mV]	R_p [Ω/cm²]	CR [mm/year]
PANI-H_3PO_4	0	28	1.50×10^{-6}	21.3	18.2	2.84×10^{6}	2.22×10^{-8}
	1	-17	3.60×10^{-7}	20.1	17.6	1.13×10^{7}	5.32×10^{-9}
	5	-15	3.70×10^{-7}	20.5	17.9	1.12×10^{7}	5.47×10^{-9}
	10	-21	9.90×10^{-7}	21.2	18.1	4.28×10^{6}	1.46×10^{-8}
	15	-36	1.20×10^{-6}	28.6	26.9	5.02×10^{6}	1.77×10^{-8}
PANI-H_2SO_4	0	28	1.50×10^{-6}	21.3	18.2	2.84×10^{6}	2.22×10^{-8}
	1	-16	3.10×10^{-7}	20.1	17.6	1.31×10^{7}	4.58×10^{-9}
	5	-18	4.60×10^{-7}	20.3	16.3	8.53×10^{7}	6.21×10^{-9}
	10	-18	9.20×10^{-7}	20.9	16.5	4.35×10^{6}	1.36×10^{-8}
	15	-32	2.10×10^{-6}	26.9	24.2	2.63×10^{6}	3.10×10^{-8}
PANI-HCl	0	28	1.50×10^{-6}	21.3	18.2	2.84×10^{6}	2.22×10^{-8}
	1	-14	3.30×10^{-7}	21.9	17.9	1.30×10^{7}	4.88×10^{-9}
	5	-15	3.80×10^{-7}	21.5	16.2	1.06×10^{7}	5.62×10^{-9}
	10	-14	9.50×10^{-7}	20.8	15.8	4.10×10^{6}	1.40×10^{-8}
	15	-25	1.70×10^{-6}	25.6	26.3	3.31×10^{6}	2.51×10^{-8}
PANI-PTSA	0	28	1.50×10^{-6}	21.3	18.2	2.84×10^{6}	2.22×10^{-8}
	1	-16	2.80×10^{-7}	21.6	18.3	1.54×10^{7}	4.14×10^{-9}
	5	-17	3.90×10^{-7}	22.0	18.1	1.11×10^{7}	5.77×10^{-9}
	10	-22	9.10×10^{-7}	21.8	17.9	4.69×10^{6}	1.35×10^{-8}
	15	-28	2.10×10^{-6}	26.3	25.6	2.68×10^{6}	3.10×10^{-8}
PANI-SSA	0	28	1.50×10^{-6}	21.3	18.2	2.84×10^{6}	2.22×10^{-8}
	1	-19	2.80×10^{-7}	21.1	18.6	1.53×10^{7}	4.14×10^{-9}
	5	-18	4.10×10^{-7}	20.8	18.4	9.63×10^{7}	6.06×10^{-9}
	10	-21	9.80×10^{-7}	20.5	17.8	4.22×10^{6}	1.45×10^{-8}
	15	-25	1.90×10^{-6}	27.1	24.8	2.96×10^{6}	2.81×10^{-8}

All the parameters are given as arithmetic averages within 5 measured values.

3.13. Mechanism of corrosion protection by polyaniline coatings.

The mechanism of metal passivation may be due to the redox catalytic effect of PANI. Iron is directly oxidised to a ferric state while ferric oxide is formed and acts as a passivating layer. This direct oxidation process is accelerated by PANI which provides ferric oxide rather than ferrous oxide. Ferrous oxide has higher water solubility.[45, 46]

Dissolution of Fe and formation of soluble Fe^{2+} ions as anodic process:

$$2\,Fe \rightarrow 2\,Fe^{2+} + 4e^{-} \quad (4)$$

Cathodic process involves with O_2 reduction and the reduction of PANI:

$$O_2 + 2\,H_2O + 4e^{-} \rightarrow 4\,OH^{-} \quad (5)$$

$$(PANI^{y+}A_y^{-})_n + nye^{-} \rightarrow (PANI)_n + nyA^{-} \quad (6)$$

Where A^- (for example from PANI-HCl) is Cl^-

chemical process:

$$2\,Fe^{2+} + 4\,OH^{-} \rightarrow 2\,Fe(OH)_2 \xrightarrow{+OH^{-}} 2Fe(OH)_3 \xrightarrow[-3H_2O]{} Fe_2O_3 \quad (7)$$

4. Conclusion

Polyaniline salts were synthesized and described and the feasibility of their use as pigments for organic coatings was investigated. The polyaniline salts were studied by thermal analysis (TGA and DSC), and nearly identical results were obtained for all of them. Also, the results of the two thermal methods were in mutual agreement. Furthermore, the polyaniline salts were assessed by XRD, which provided the evidence that all the polyaniline salts showed a slight degree of crystallinity. FTIR spectroscopy was also used to study the salts. The spectra exhibited bands characteristic of the respective polyaniline salts and, in addition, revealed incomplete protonation of two polyaniline salts, which was also manifested by lower electrical conductivities. Electrical conductivities were measured in aqueous extracts of the salts. It was concluded that the electrical conductivity may have been affected by the molecular weight of the polyaniline salt (determined by SEC/GPC in NMP). Particle size (expressed as the diameter of an equivalent sphere) was also measured for the polyaniline salts. No appreciable differences were observed in the particle sizes of the polyaniline salts. The morphology of the polyaniline salt particles was examined by electron microscopy, which revealed that the particles had an isometric shape and formed clusters. The acidity and electrical conductivity of 10 wt% suspensions of the salts in redistilled water were measured, and a substantial increase in both parameters was observed. This can be explained by deprotonation of the salts. The stability of the polyaniline salts in the alkyd resin was tested prior to formulating the coatings. The results demonstrate that none of the polyaniline salts is converted to the polyaniline base in this binder; instead, all of them remain in their salt form and do not affect adversely the binder stability. Similarly, the dopant type had no effect on the mechanical resistance values in the mechanical tests. Mechanical resistance was only poorer if the pigment volume concentration was increased to the highest level, PVC = 15 %, which is roughly one-half of the critical pigment volume concentration. The highest corrosion resistance of the organic coatings was observed at PVC = 1 % or 5 % also in the accelerated corrosion tests. The highest anticorrosion efficiency after the cyclic corrosion tests was observed with the organic coating containing pigment PANI - SSA (PVC = 5 %). Likewise this organic coating has shown maximum value of polarization resistance and very low value of corrosion rate measured by the method of potentiodynamic polarization

Acknowledgment

The financial support of Czech Science Foundation (16-02787S) is gratefully acknowledged.

References

[1] Abaci, U, Guney, HY, Kadiroglu, U, "Morphological and electrochemical properties of PPy, PAni bilayer films and enhanced stability of their electrochromic devices (PPy/PAni–PEDOT, PAni/PPy–PEDOT)." Electrochimica Acta, **95** 214–224 (2013)

[2] Somboonsub, B, Srisuwan, S, Invernale, MA, Thongyai, S, Praserthdam, P, Scola, DA, Sotzing, GA, "Comparison of the thermally stable conducting polymers PEDOT, PANi, and PPy using sulfonated poly(imide) templates." Polymer, **51** 4472–4476 (2010)

[3] Stejskal, J, "Polymers of phenylenediamines." Progress in Polymer Science, **41** 1–31 (2015)

[4] Sanches, EA, Silva, JMS, Ferreira, JMO, Soares, JC, Santos, AL, Trovati, G, Fernandes EGR, Mascarenhas, YP, "Nanostructured Polyaniline Emeraldine-base form (EB-PANI), a structural investigation for different neutralization times." Journal of Molecular Structure, **1074** 732–737 (2014)

[5] Jamadade, VS, Dhawale, DS, Lokhande, CD, "Studies on electrosynthesized leucoemeraldine, emeraldine and pernigraniline forms of polyaniline films and their supercapacitive behavior." Synthetic Metals, **160** 955–960 (2010)

[6] Blinova, NV, Stejskal, J, Trchová, M, Prokeš, J, "Polyaniline prepared in solutions of phosphoric acid, Powders, thin films, and colloidal dispersions." Polymer, **47** 42–43 (2006)

[7] Stejskal, J, Kratochvíl, P, Helmstedt, M, "Polyaniline Dispersions. 5. Poly(vinyl alcohol) and Poly(*N*-vinylpyrrolidone) as Steric Stabilizers." Langmuir, **12** 3389–3392 (1996)

[8] Campos, TLA, Kersting, DF, Ferreira, CA, "Chemical synthesis of polyaniline using sulphanilic acid as dopant agent into the reactional medium." Surface and Coatings Technology, **122** 3–5 (1999)

[9] Ding, L, Wang, X, Gregory, RV, "Thermal properties of chemically synthesized polyaniline (EB) powder." Synthetic Metals, **104** 73–78 (1999)

[10] Bhadra, S, Khastgir, D, "Degradation and stability of polyaniline on exposure to electron beam irradiation (structure–property relationship)." Polymer Degradation and Stability, **92** 1824–1832 (2007)

[11] Shumakovich, G, Kurova, V, Vasil'eva, I, Pankratov, D, Otrokhov, G, Morozova, O, Yaropolov, A, „Laccase-mediated synthesis of conducting polyaniline." Journal of Molecular Catalysis B: Enzymatic, 77 105–110 (2012)

[12] Siva, T, Kamaraj, K, Sathiyanarayanan, S, "Epoxy curing by polyaniline (PANI) – Characterization and self-healing evaluation." Progress in Organic Coatings, **77** 1095–1103 (2014)

[13] Pereira, VR, Isloor, AM, Bhat, UK, Ismail, AF, "Preparation and antifouling properties of PVDF ultrafiltration membranes with polyaniline (PANI) nanofibers and hydrolysed PSMA (H-PSMA) as additives." Desalination, **351** 220–227 (2014)

[14] Gedela, VR, Srikanth, VVSS, "Electrochemically active polyaniline nanofibers (PANi NFs) coated graphene nanosheets/PANi NFs composite coated on different flexible substrates." Synthetic Metals, **193** 71–76 (2014)

[15] Kulkarni, MV, Kale, BB, "Studies of conducting polyaniline (PANI) wrapped-multiwalled carbon nanotubes (MWCNTs) nanocomposite and its application for optical pH sensing." Sensors and Actuators B: Chemical, **187** 407–412 (2013)

[16] Ozyilmaz, AT, Akdag, A, Karahan, IH, Ozyilmaz, G, "The influence of polyaniline (PANI) coating on corrosion behaviour of zinc–cobalt coated carbon steel electrode." Progress in Organic Coatings, **76** 993–997 (2013)

[17] Abu-Thabit, NY, Makhlouf, ASH, Handbook of Smart Coatings for Materials Protection 17 – Recent advances in polyaniline (PANI)-based organic coatings for corrosion protection, (2014)

[18] Armelin, E, Alemán, C, Iribarren, JI, "Anticorrosion performances of epoxy coatings modified with polyaniline, A comparison between the emeraldine base and salt forms." Progress in Organic Coatings, **65** 88–93 (2009)

[19] Akbarinezhad, E, Ebrahimi, M, Sharif, F, Attar, MM, Faridi, HR, "Synthesis and evaluating corrosion protection effects of emeraldine base PAni/clay nanocomposite as a barrier pigment in zinc-rich ethyl silicate primer." Progress in Organic Coatings, **70** 39–44 (2011)

[20] Wessling, B, "Scientific and commercial breakthrough for organic metals." Synthetic Metals, **85** 1313–1318 (1997)

[21] Kohl, M, Kalendová, A, "Effect of polyaniline salts on the mechanical and corrosion properties of organic protective coatings." Progress in Organic Coatings, **86** 96–107 (2015)

[22] Figueira, RB, Silva, CJR, Pereira, EV, "Hybrid sol-gel coatings for corrosion protection of galvanized steel in simulated concrete pore solution." Journal of Coatings Technology and Research, **13** (2) 355**–**373 (2016)

[23] Mahato, N, Cho, MH, "Graphene integrated polyaniline nanostructured composite coating for protecting steels from corrosion: Synthesis, characterization, and protection mechanism of the coating material in acidic environment." Construction and Building Materials, **115** 618–633 (2016)

[24] Veselý, D, Kalendová, A, "Anticorrosion efficiency of $Zn_xMg_yAl_2O_4$ core–shell spinels in organic coatings." Progress in Organic Coatings, **62** 5–20 (2008)

[25] Goldschmidt, A, Streitberger, HJ, BASF handbook on basics of coating technology, Vincentz Network, Hannover, Germany (2007) ISBN 973-3-86630-903-6

[26] Kalenda, P, Kalendová, A, Štengl, V, Antoš, P, Šubrt, J, Kváča, Z, Bakardjieva, S, "Properties of surface-treated mica in anticorrosive coatings" Progress in Organic Coatings, **49** 137–145 (2004)

[27] Al-Ahmed, A, Mohammad, F, Rahman, MZA, "Preparation, characterization, thermooxidative degradation, and stability of polyaniline/polyacrylonitrile composites in terms of direct-current electrical conductivity retention." Journal of Applied Polymer Science, **99** 437–448 (2006)

[28] Gök, A, Omastová, M, Prokeš, J, "Synthesis and characterization of red mud/polyaniline composites, Electrical properties and thermal stability." European Polymer Journal, **43** 2471–2480 (2007)

[29] Ding, L, Wang, X, Gregory, RV, "Thermal properties of chemically synthesized polyaniline (EB) powder." Synthetic Metals, **104** 73–78 (1999)

[30] Sathiyanarayanan, S, Azim, SS, G. Venkatachari, G "Corrosion resistant properties of polyaniline–acrylic coating on magnesium alloy." Applied Surface Science, **253** 2113–2117 (2006)

[31] Han, D, Chu, Y, Yang, L, Liu, Y, Lv, Z, "Reversed micelle polymerization: a new route for the synthesis of DBSA–polyaniline nanoparticles." Colloids and Surfaces A: Physicochemical and Engineering Aspects, **259** 179–187 (2005)

[32] Stejskal, J, Trchová, M, "Aniline oligomers versus polyaniline." Polymer Internaional, **61** 240–251 (2012)

[33] Arasi, JY, Jeyakumari, JJL, Sundaresan, B, Dhanalakshmi, V, Anbarasan, R, "The structural properties of poly(aniline)–analysis via FTIR spectroscopy." Spectrochimica Acta Part A, Molecular and Biomolecular Spectroscopy, **74** 1229–1234 (2009)

[34] Stejskal, J, Trchová, M, Brodinová, J, Kalenda, P, Fedorova, SV, Prokeš, J, Zemek, J, "Coating of zinc ferrite particles with a conducting polymer, polyaniline." Journal of Colloid and Interface Science, **298** 87–93 (2006)

[35] Trchová, M, Stejskal, J, "Polyaniline, The infrared spectroscopy of conducting polymer nanotubes (IUPAC Technical Report)." Pure and Applied Chemistry, **83** 1803–1817 (2011)

[36] Chapman, CA, Thirlwell, EL, "Spectra of phosphorus compounds-I the infra-red spectra of orthophosphateS." Spectrochimica Acta, **20** 937–947 (1964)

[37] Socrates, G, Infrared and Raman characteristic group frequencies, Tables and charts, 3rd Ed., Wiley, Londýn, Anglie; (2004) ISBN, 978-0-470-09307-8.

[38] Stejskal, J, Riede, A, Hlavatá, D, Prokeš, J, Helmstedt, M, Holler, P, "The effect of polymerization temperature on molecular weight, crystallinity, and electrical conductivity of polyaniline." Synthetic Metals, **96** 55–61 (1998)

[39] Trchová, M, Matějka, P, Brodinová, J, Kalendová, A, Prokeš, J, Stejskal, J, "Structural and conductivity changes during the pyrolysis of polyaniline base." Polymer Degradation and Stability, **91** 114–121 (2006)

[40] Kalendová, A, Sapurina, I, Stejskal, J, Veselý, D, "Anticorrosion properties of polyaniline-coated pigments in organic coatings." Corrosion Science, **50** 3549–3560 (2008)

[41] Gorkum, R, Bouwman, E, "The oxidative drying of alkyd paint catalysed by metal complexes." Coordination Chemistry Reviews, **249** 1709–1728 (2005)

[42] Kalendová, A, Veselý, D, Kohl, M, Stejskal, J, "Anticorrosion efficiency of zinc-filled epoxy coatings containing conducting polymers and pigments." Progress in Organic Coatings, **78** 1–20 (2015)

[43] Kalendová, A, Veselý, D, "Study of the anticorrosive efficiency of zincite and periclase-based core–shell pigments in organic coatings." Progress in Organic Coatings, **64** 5–19 (2009)

[44] Samui, AB, Patankar AS, Rangarajan, J, Deb, PC, "Study of polyaniline containing paint for corrosion prevention." Progress in Organic Coatings, **47** 1–7 (2003)

[45] Zhao, Y, Zhang, Z, Yu, L, "Corrosion protection of carbon steel by electrospun film containing polyaniline microfibers." Reactive and Functional Polymers, **102** 20–26 (2016)

[46] Rout, TK, Jha, G, Singh, AK, Bandyopadhyay, N, Mohanty, ON, "Development of conducting polyaniline coating: a novel approach to superior corrosion resistance." Surface and Coatings Technology, **167** 16–24 (2003)